

Microbiologically influenced corrosion on rails

S. Maruthamuthu^{1,*}, T. Nagendran¹, B. Anandkumar², M. S. Karthikeyan¹,
N. Palaniswamy¹ and G. Narayanan³

¹Corrosion Protection Division, Central Electrochemical Research Institute (CSIR), Karaikudi 630 006, India

²Corrosion Science and Technology Division, Indira Gandhi Centre for Atomic Research, Kalpakkam 603 102, India

³Southern Railway, General Manager's Office, Chennai 600 003, India

Corrosion of rails has been a cause of concern for the Southern Railways. Out of many causes, corrosion due to toilet droppings is more pronounced. In this study, the role of bacteria, viz. heterotrophic bacteria, manganese oxidizers, iron bacteria and ureolytic bacteria on rails have been studied. The attachment of rod- and cocci-shaped bacteria were noticed on the corroded rail sample. A porous rust layer and fine cracks were noticed on the steels. Twenty bacterial strains were identified by molecular technique and most of the bacteria were positive in citrate and urease test, where 85% species could tolerate high pH 9.0. X-ray photoelectron spectroscopy revealed that FeOOH in the bare steel was converted to ferric oxides and hydroxides due to bacterial corrosion. When the rail sample was tested at low AC perturbations, the biofilm provided protection to the rails. However, at higher anodic potentials, the biofilm was not able to protect the bare material. It could be assumed that the ureolytic bacteria and iron/manganese oxidizers may create differential pH gradient on the metal surface which enhances the electrochemical reaction of the metal surface.

Keywords: Atmospheric corrosion, bacterial corrosion, rail corrosion, ureolytic bacteria.

CORROSION of rails causes premature renewals (<http://www.iitk.ac.in/infocell/iitk/newhtml/storyoftheweek60.html>). The most common form of corrosion of rails is atmospheric corrosion. The corrosion rate along the rail base is affected by humidity and deposited salts, but most importantly by stray DC currents that generate electrolytic reactions. Electrolytic reactions increase galvanic corrosion effects and corrosion rates considerably¹. The frequency of wetting and drying determine the severity of atmospheric corrosion. Pollutants, viz. trace elements, chloride, sulphate, etc. and contaminants, viz. microbes in the environment dictate the severity of atmospheric corrosion². The rails laid near coastal regions are more prone to atmospheric corrosion (<http://www.iitk.ac.in/infocell/iitk/newhtml/storyoftheweek60.html>) warranting more frequent replacement of rails. The rail stretches used for halting early morning trains near major junctions and stoppages show pronounced corrosion at bottom flanges

and fittings. Railway officials and corrosion engineers believe that the corrosion is caused by microbes present in human wastes. Intense corrosion takes place at these locations (i.e. under the liner) due to accumulation of moisture from the atmosphere and discharge from the open toilets of the railway coaches. Human urine contains 0.4–0.5 M urea which results in an annual release of 10 kg of urea per adult³. It is also well known that many ureolytic microorganisms are present in human wastes which hydrolyse urea into carbonic acid and ammonia. The hydrolysis of urea is catalysed by urease enzyme³. But no study has been carried out on the impact of urine on corrosion. No evidence has been proposed on microbiologically influenced corrosion (MIC) on rails. In this study, role of bacteria on rail corrosion was studied. Some bacteria, viz. heterotrophic bacteria, manganese oxidizers, iron bacteria and ureolytic bacteria have been isolated and corrosion behaviour of rails have also been studied by using synthetic urine with bacteria isolated from rails.

Materials and methods

Collection site

Corrosion product from a steel rail was taken from a track close to a major junction and tested exhaustively. The corrosion products were scraped from rails, elastic rail clip (ERC), rail insert (RIT) and under the liner (ULR) (Figure 1) by using sterile knife and collected separately in sterile saline containers. The corrosion products for chemical analysis were kept in an ice box, and transported from the site to Central Electrochemical Research Institute (CECRI), Karaikudi.



Figure 1. Elastic rail clip, liner and insert with rail.

*For correspondence. (e-mail: biocorrcecri@gmail.com)

Material selection

The specimens (grade 880 rail steel) for this study were supplied by the Southern Railways. The composition of grade 880 steel is as follows. Carbon: 0.60–0.80%, manganese: 0.80–1.30%, sulphur: 0.10–0.50%, phosphorus: 0.05 max, silica: 0.05 max, iron: balance.

Physical and chemical analysis

pH: The corrosion product collected from the rail was agitated in deionized water. The pH was measured at room temperature using a digital pH meter: Eutech instruments model: pH 510 (pH/mV/°C meter).

Chemical and surface analysis

Chloride and sulphate were estimated by Mohr's method and gravimetric method respectively. 250 mg of sample was mixed with 50 ml of acid mixture (4:1 supra pure nitric acid and perchloric acid). The mixture was heated on a hot plate until the mixture was condensed to 1 ml. Triple distilled water (25 ml) was added to this mixture, filtered and was analysed in atomic absorption spectroscopy. The dried corrosion products and bare rail were taken and spectra were recorded between 4000 and 400 cm^{-1} wave numbers on a Perkin Elmer, UK Paragon 500 model Fourier transform infrared spectroscopy (FTIR) with 16 scan speed. The samples were mixed with spectroscopically pure KBr and pelletized in the ratio of 1:100. The pellets prepared were fixed in the sample holder and the analysis was carried out. The corrosion products were dried at 60°C and subjected to X-ray diffraction (XRD) analysis. X'pert PRO PAN analysed X-ray diffractometer with Syn Master 793 software to identify the corrosion product. The XRD pattern was recorded using a computer-controlled XRD-system, JEOL, and model: JPX-8030 with $\text{CuK}\alpha$ radiation (Ni filtered = 13418 Å) at the range of 40 kV, 20 A. The 'peak search' and 'search match' program built-in software (syn master 7935) was used to identify the peak table and ultimately for the identification of XRD peak. The X-ray photoelectron spectroscopy (XPS) measurements were performed to obtain information about the elements in corrosion product and bare rail steel. The XPS spectrum was taken by ESCA model VG 3000 system. The base pressure in the experimental chamber was in the low 10^{-9} mbar range. The spectrum was collected using $\text{MgK}\alpha$ (1253.6 eV) radiation and the overall energy resolution was about 0.8 eV. Samples of 0.6 cm^2 were used. Survey spectrum was recorded for the samples in the 0–1100 eV kinetic energy by 1 eV steps whereas high resolution scan with 0.1 eV steps were conducted over the following regions of interest: Fe2p, C1s, O1s. The corrosion products were finely powdered and analysed by XPS. The bacterial

attachment on corroded rails and surface morphological characteristics of the corroded rail steels were observed under a scanning electron microscope (SEM; Hitachi model S-3000H). The sample was fixed for 12 h at room temperature with 3% glutaraldehyde and 4% paraformaldehyde in 0.1 M phosphate buffer solution (pH 7.2). The coupons were dehydrated using different concentrations of ethanol solution 25%, 50%, 75% and 100% and finally degreased with acetone. The coupons were air-dried and sputter-coated with gold using ion sputters. The coupons were examined at different magnifications (4.0, 5.0 and 9.0 K) by SEM.

Bacterial enumeration and identification

Isolation of bacteria: Corrosion product (1 g) from rail was removed aseptically and transferred to 99 ml of sterile deionized water. It was subjected to serial dilution and plated by using nutrient agar, Mn agar base, isolation medium for iron bacteria, *Thiobacillus* agar and urea agar base by pour plate method and for sulphate reducing bacteria (SRB) medium by using most probable number technique. The plates were incubated at 37°C for 24–48 h and 22 days for SRB. The total viable bacterial counts were enumerated and the bacterial population was expressed as colony forming units per gram (CFU/g).

Partial biochemical characterization of the isolates: Morphologically dissimilar dominating isolated colonies were selected randomly. Further they were streaked on nutrient agar, Mn agar base, isolation medium for iron bacteria, urea agar base plates and purified. The pure cultures were maintained in agar slants at 4°C to keep the microbial strain viable. The dissimilar aerobic bacteria isolated from medium were identified according to *Bergey's Manual of Determinative Bacteriology*⁴. The isolated bacterial strains were identified up to genus level by their morphological and partial biochemical characterization. Biochemical characterization of the isolates was carried out by employing Himedia biochemical test kit (Mumbai). The adaptation of bacteria with various environment factors such as temperature, pH and chloride concentration was tested.

Molecular identification of the bacteria: Genomic DNA of the bacterial isolates was extracted according to Ausubel *et al.*⁵. Amplification of gene encoding small subunit ribosomal RNA was carried out using eubacterial 16s rRNA primers (forward primer 5'-AGAGTTTGA-TCCCTGGCTGAG-3' *E. coli* position 8–27 and reverse primer 5'-ACGGCTACCTTGTTACGACTT-3' *E. coli* positions 1494–1513)⁶. Polymerase chain reaction (PCR) was performed with a 50 μl reaction mixture containing 2 μl of DNA as template, each primer at a concentration of 0.5 μM and 1.5 mM MgCl_2 and each dNTP at a

concentration 50 μM as well as 1 unit of *Taq* DNA polymerase and buffer as recommended by the manufacturer (MBI Fermentas). PCR was carried out with a master cycler personal (Eppendorf) with the following programme. Initial denaturation at 95°C for 1 min, 40 cycles of denaturation (3 min at 95°C), annealing (1 min at 55°C) and extension (2 min at 72°C); followed by a final extension at (72°C). The amplified product was purified using GFX™ PCR DNA and gel-based purification kit (Amersham Biosciences) and cloned in pT257R/T vector according to the manufacturer's instruction (InsTA clone™ PCR product cloning kit, MBI Fermentas) and transformants were selected on Luria-Bertani (LB) medium containing Ampicillin 100 $\mu\text{g/ml}$ and X gal 80 $\mu\text{g/ml}$.

Phylogenetic analysis of the isolates: The sequences obtained were analysed with BLAST search version 2.2.20 (ref. 7) and tools of Ribosomal Database Project II Release 10 (<http://rdp.cme.msu.edu>) for taxonomic hierarchy of the sequences. Multiple sequence alignments were performed using CLUSTAL X2 (ref. 8) with a collection of taxonomically related sequences obtained from the National Centre for Biotechnology Information (NCBI) Taxonomy Homepage (<http://www.ncbi.nlm.nih.gov/Taxonomy/taxonomyhome.html/>) and Ribosomal Database Project-II Release 10 (<http://rdp.cme.msu.edu>). Phylogenetic and similitude analyses were done with the common 16S rRNA gene regions, and all alignment gaps were treated as missing data. The paired similitude and pairwise distance calculations using the transversion/transition weighting ($R = s/v$) and the Kimura two-parameter model⁹ were performed with the MEGA version 4.1 program¹⁰. Phylogenetic trees were constructed (neighbour-joining method), and 1000 bootstrap replications were carried out to validate internal branches¹¹. Mat GAT v. 2.01 software¹² was used to calculate the similitude percentages among sequences.

Corrosion studies

Electrolyte selection: Synthetic urine¹³ was used as an electrolyte; 1 litre of medium contains $\text{CaCl}_2 \cdot 2\text{H}_2\text{O}$ – 0.651 g, $\text{MgCl}_2 \cdot 6\text{H}_2\text{O}$ – 0.651 g, NaCl – 4.6 g, Na_2SO_4 – 2.3 g, KH_2PO_4 – 2.8 g, KCl – 1.6 g, NH_4Cl – 1.0 g, urea – 25.0 g, creatinine – 1.1 g and trypticase soy broth – 10.0 g at pH 5.8.

Weight loss measurements: Mild steel grade 880 rail steel coupons of size 2.5 cm \times 2.5 cm \times 0.6 cm were mechanically polished to mirror finish and then degreased using trichloroethylene. In this study, 500 ml of synthetic urine without urea and bacteria was used as the control system, whereas 500 ml synthetic urine with urea and mixed culture isolated from corroded rails was used as

the experimental system. The coupons were immersed for 30 days in both the systems for weight loss measurements¹⁴.

Electrochemical studies

Polarization studies: A rail steel coupon was mounted in araldite with an exposure area of 1 \times 1 cm² dimension as a working electrode used for polarization studies. Specimens were mechanically polished to mirror finish and degreased with trichloroethylene followed by deionized water. Specimen was immersed in a separate 250 ml conical flask containing synthetic urine medium. The medium without urea and bacteria was used as a control system. Polarization measurements were carried out using PARSTAT 2273 Princeton Applied Research by using POWER SINE and POWER CORR software, employing a platinum electrode, saturated calomel electrode as reference electrode and the rail steel metal as working electrode. The system was allowed to attain a steady potential value for 10 min. The polarization curves were obtained by scanning from open circuit potential towards 200 mV anodically and cathodically on the 7th day. The scan rate was 120 mV/min (ref. 15).

Impedance studies: Electrodes of the same specification employed in polarization studies were also used for impedance studies. Impedance measurements were carried out using PARSTAT 2273 Princeton Applied Research by using POWER SINE and POWER CORR software. Impedance measurements were taken on the 7th day. After attainment of steady state, an AC signal of 10 mV amplitude was applied and impedance values were measured for frequencies ranging from 0.1 Hz to 100 kHz. The values of R_{ct} were obtained from Nyquist plot.

Results and discussion

Chemical characteristics of corrosion products

pH and chloride: The pH and concentration of adsorbed chloride in different rail materials are presented in Table 1. The pH of the corrosion product collected from RIT was 8.17. The pH of corrosion product from rail was

Table 1. Concentration of chloride and pH of corrosion product collected from rails

Corrosion product	pH	Chloride (mg/kg)	Sulphate (mg/kg)
Under the liner (ULR)	8.0	4860	Nil
Corrosion product from rails	7.84	4860	Nil
Rail insert (RIT)	8.17	7120	Nil

Table 2. Distribution of different elements in rail corrosion products

Sample	Fe	Mn	Ca	Cu	Cr	Zn
Elastic rail clip (ERC) (mg/kg)	440,825	3962	972	414	140	71
RIT (mg/kg)	422,425	2650	802	203	49	30

Table 3. Total viable count on corroded rails collected from a railway junction

Sample	Heterotrophic bacteria (CFU/g)	Iron bacteria (CFU/g)	Manganese oxidizing bacteria (CFU/g)	Ureolytic bacteria (CFU/g)	<i>Thiobacillus</i> (acid producers) (CFU/g)	Sulphate reducing bacteria (CFU/g)
Corrosion product from rail	5.2×10^7	10.6×10^7	7.8×10^5	5×10^4	Nil	Nil
ERC	6.7×10^8	6.8×10^7	5.3×10^7	6.8×10^4	Nil	Nil
RIT	TNTC	13.3×10^6	6.3×10^6	13.4×10^5	Nil	Nil
ULR	13.2×10^7	7.3×10^6	4.7×10^6	8.6×10^5	Nil	Nil

7.84, whereas for the corrosion product of the ULR pH was about 8.0. The adsorbed chloride concentration in the rail corrosion product from RIT was 7120 mg/kg or 0.712%. The chloride concentration in corrosion product from rail and ULR was 4860 mg/kg. The alkaline pH of the corrosion product is due to the bacterial activity on the surface of the rail. The adsorbed chloride concentration in the rail corrosion product was somewhat higher which may be due to the adsorption of human excretory products. The sulphate concentration of the corrosion product was nil. This result indicates that the adsorption of chloride is one of the culprits of corrosion.

Concentration of various trace metals

The distribution of different elements in rail corrosion product is presented in Table 2. Iron content was higher in the corrosion product where manganese concentration was also about in the range from 2650 to 3962 mg/kg. Besides calcium, copper, chromium and zinc were also noticed in the corroded rail materials. It can be assumed that manganese and iron leach out from the rail steel due to corrosion. Atmospheric calcium, copper, chromium and zinc may be settled on the rail steel which determine the electrochemical behaviour.

Bacterial observation on corrosion product

Figure 2 shows the attachment of bacteria on corroded rail materials observed through SEM. Rod- and cocci-shaped bacteria were noticed on corroded steel. The rust layer was porous in nature and appeared to be loose. Compact regions were not seen on the rust surface of the rail steel¹⁶. Fine cracks could be observed (Figure 2a) which supports the observations made by Panda *et al.*¹⁶ on steel in the salt fog experiment. The enumeration of heterotrophic bacteria, iron bacteria, manganese oxidizers and ureolytic bacteria are presented in Table 3. The count

of heterotrophic bacteria, iron bacteria, manganese oxidizers and ureolytic bacteria on corrosion product from rail was 5.2×10^7 , 10.6×10^7 , 7.8×10^5 and 5×10^4 CFU/g respectively. The count of heterotrophic bacteria, iron bacteria, manganese oxidizers and ureolytic bacteria on ERC was 6.7×10^8 , 6.8×10^7 , 5.3×10^7 and 6.8×10^4 CFU/g respectively. The count of heterotrophic bacteria, iron bacteria, manganese oxidizers, and ureolytic bacteria on RIT was TNTC (too numerous to count), 13.3×10^6 , 6.3×10^6 and 13.4×10^5 CFU/g respectively. The count of heterotrophic bacteria, iron bacteria, manganese oxidizers and ureolytic bacteria on ULR was 13.2×10^7 , 7.3×10^6 , 4.7×10^6 and 8.6×10^5 CFU/g respectively.

The results indicate the absence of acid producers and SRB. It can be assumed that the alkalinity on the surface of the rail suppresses the proliferation of acid producers and SRB. Most of the bacteria are positive in citrate and urease tests where 100% of the isolated bacteria (20 isolates) produce catalase, which does not allow the reduction of pH by peroxide on the material. It should be considered that most of the urease positive strains precipitate calcium by hydrolysis of urea. This result supports the previous observations made by Braissant *et al.*¹⁷ and Knorre and Krumbein¹⁸, who noticed that the urease positive strains are calcium precipitating bacteria. The observation supports the high pH of the corrosion product which is due to the bacterial activity. The role of catalase enzyme and activity of ureolytic bacteria by production of ammonia also suppresses the acid producers on the surface of the rails. The study also reveals that all ureolytic strains can grow at temperatures up to 40°C, about 55% of identified species can tolerate low pH 3 and 85% species can tolerate at high pH 9. The surface temperature of the rails was between 34°C and 45°C from 09:00 a.m. to 02:00 p.m. It can be concluded that the activity may be suppressed above 40°C, but inhibition of bacterial proliferation is difficult at 45°C on the rail surface. The temperature fluctuations and frequency of wet and dry conditions on the surface determine the activity

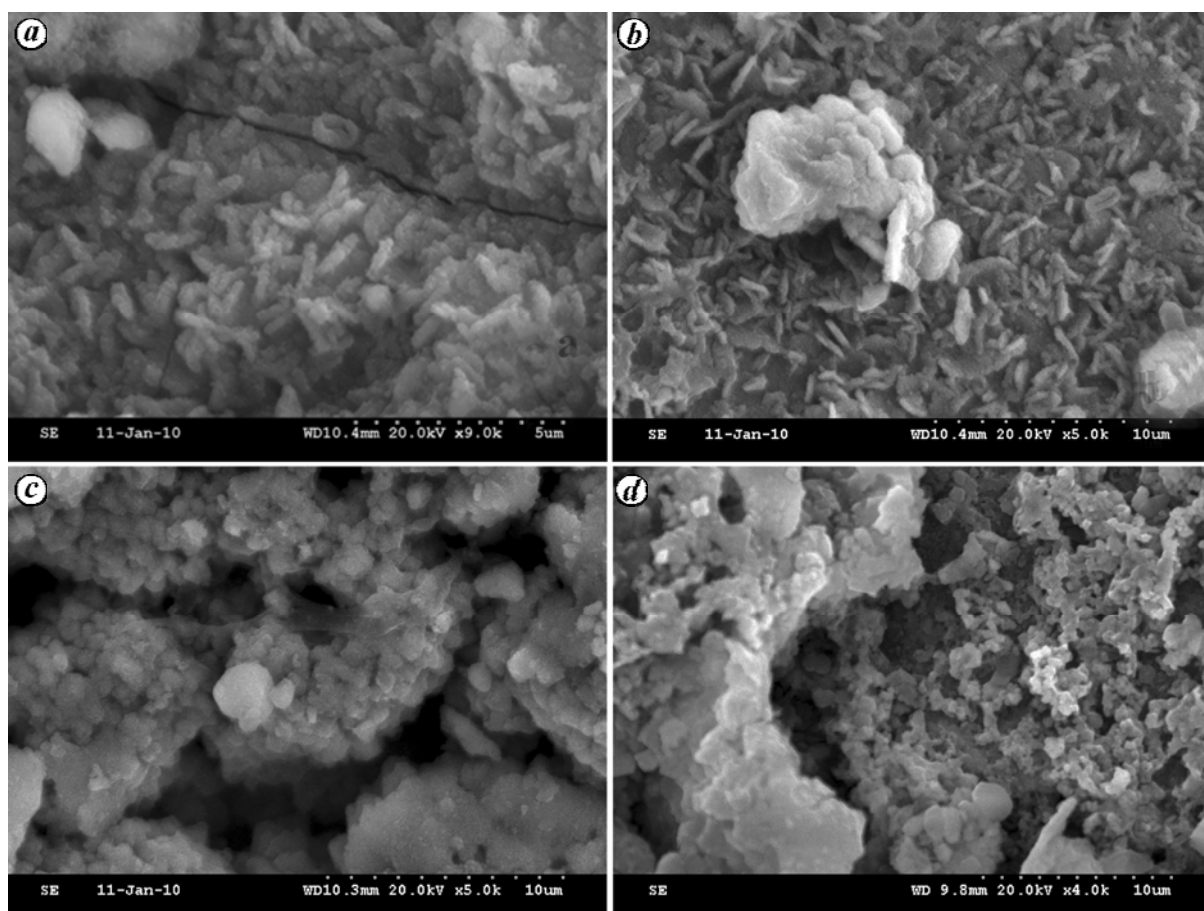


Figure 2a-d. Bacterial attachment on corroded rails. *a*, Attachment of rod-shaped bacteria. *b*, Attachment of rod-shaped bacteria and calcium precipitating bacteria. *c*, *d*, Attachment of cocci-shaped bacteria.

of microbes. Besides, most bacteria can grow in concentrations up to 10,000 ppm of chloride. It can be inferred that ureolytic bacteria hydrolyse urea and produce carbonic acid and ammonia³. The ammonia produces high pH on the metal surface and encourages low crystalline form of iron oxide. Subsequently, bacteria accumulate calcium and magnesium in their cell wall. This concept was supported by the presence of calcium in the corrosion product.

Molecular identification and phylogenetic analysis of the isolates

Twenty bacterial isolates were identified by molecular identification with 16S rDNA sequencing. The sequences obtained were submitted to a Basic Local Alignment Search Tool (BLAST) search to retrieve the corresponding phylogenetic relatives. The phylogenetic affiliations (Firmicutes and Proteobacteria) were confirmed by analyses of all related species recognized by the taxonomic and classification hierarchy done with the NCBI Taxonomy Homepage and Ribosomal Database Project-II Release 10. Two neighbour-joining phylogenetic trees were constructed for the Firmicutes (Figure 3) and Proteobacteria (Figure 4) to analyse the relationships among

the sequences of the ribosomal library and related organisms from the GenBank database.

In the Firmicutes tree, all the isolates belonging to *Bacillus* genus exhibited a high nucleotide sequence similarity with *B. cereus* (99.5%), *B. subtilis* (99%), *B. litoralis* (98.5%) and *B. thuringiensis* (98%).

In the proteobacteria-related tree, eight isolates; four each belonging to *Pseudomonas* genus (*P. stutzeri*, *P. alcaligenes*, *P. acetoxians* and *P. fluorescens*) and *Serratia* genus (*S. ureilytica* and *S. marcescens*) exhibited a high nucleotide sequence similarity (99%), three isolates had similarity of 98.5% with *Enterobacter* genus (*E. aerogenes*), one each of *Acinetobacter* (*Acinetobacter* sp.) and *Oxalobacter* (*Oxalobacter* sp.) exhibited a similarity of 99%.

Phylogenetic analysis of the 16S rRNA sequences showed dominance of *Bacillus* genus in the Firmicutes tree. *Serratia* and *Pseudomonas* sp. are dominant in the proteobacterial tree.

Chemical characterization

FTIR study: Figure 5a shows the FTIR spectrum for the bare rail steel. OH-stretching was noticed at 3421 cm⁻¹.

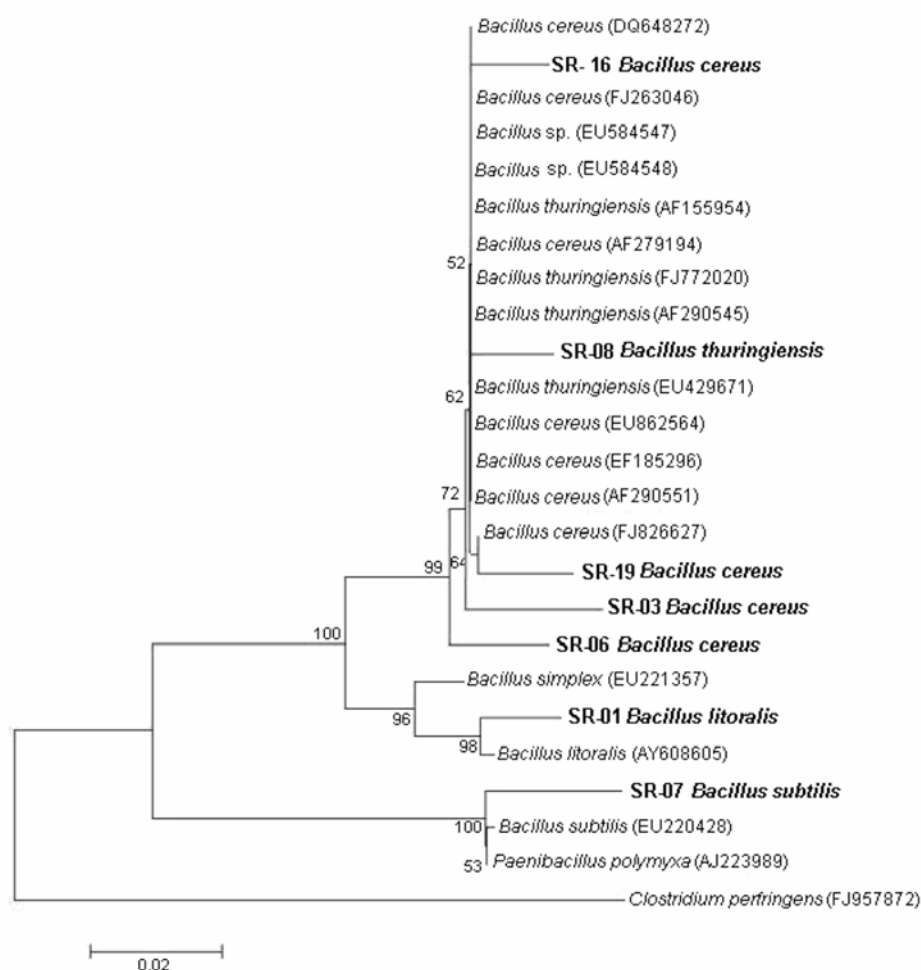


Figure 3. Neighbour-joining tree based on 16S rRNA gene sequences, showing phylogenetic relationships between sequences of the bacterial phylum Firmicutes (*Bacillus*-related species). *Clostridium perfringens* was used as a bacterial out-group. Numbers at nodes indicate bootstrap values > 50% from 1000 replicates. Accession numbers of the related GenBank sequences are given in parentheses. The isolate number and identified bacterial species are given in bold. The scale bar indicates sequence divergence.

C–H stretch was noticed at 1635 cm^{-1} . Peaks at 1635 and 789 cm^{-1} indicated the presence of $\alpha\text{-FeOOH}$ (ref. 19) on steel. A peak at 1083 cm^{-1} showed the presence of O–Fe–OH (ref. 20). Another peak at 465 indicated the presence of $\gamma\text{-Fe}_2\text{O}_3$. Figure 5 *b* and *c* shows the FTIR spectrum of corrosion rail product with peaks at 3392 cm^{-1} , indicating the presence of O–H stretching and at 2921 cm^{-1} indicating the presence of C–H stretching. A peak at 1636 cm^{-1} showed carbonyl attached with ammonium which indicates the attachment of bacterial cells on the rail. A peak at 1457 cm^{-1} showed the presence of carbonated compounds¹⁹, which indicates the role of bacterial physiology by production of carbonic acid and peaks at 1027 , 886 , 798 , 565 and 494 cm^{-1} indicating $\gamma\text{-FeOOH}$, $\alpha\text{-FeOOH}$, $\alpha\text{-FeOOH}/\gamma\text{-FeOOH}$ (ref. 17), C–Cl stretching²¹, $\gamma\text{-Fe}_2\text{O}_3$ (ref. 19) respectively. FTIR reveals the adsorption of chloride on the metal surface and the presence of organic functional group indicates the role of bacteria in corrosion. The presence of Fe_2O_3 also indicates the role

of iron bacteria on rails which convert Fe^{++} to Fe^{+++} (ref. 22).

XRD study: XRD observation of bare rail (control – without corrosion) is presented in Figure 6 *a*. A phase of FeOOH was noticed on the steel surface. An observation of the corrosion product of rail steel collected from the field is presented in Figure 6 *b* and *c*. Phases of $\text{Fe}_{21.333}\text{O}_{32}$, $\alpha\text{-Fe}_2\text{O}_3$, $\text{Fe}_{1.966}\text{O}_{2.936}$, FeO, Fe_2O_3 and FeO were noticed in the corrosion product. XRD also supports the FTIR observation and indicates the presence of major peaks of Fe_2O_3 . XRD also reveals the role of the iron bacteria in the corrosion process. Low intensity peaks of iron oxides could be identified on the corroded rails, which supports the observation made by Panda *et al.*¹⁶, who also noticed low intensity peaks on corroded rails in the salt fog experiment. This probably could be one of the reasons for poor crystalline behaviour of the rust formed in natural environment.

XPS study: The XPS analysis of bare rail is presented in Figure 7 a–c. The three important scans were done to detect the following compounds: Fe2p, C1s and O1s. Peaks at 713 and 727.1 on Fe2p scan showed the presence of Fe³⁺ (ref. 23) and FeOOH respectively. Peaks at 287.4 and 284.9 on C1s scan showed C–C and carbon²⁴ respectively. A peak at 531.5 on O1s scan showed the presence

of FeOOH²⁵. XPS analysis of the rail corrosion product is presented in Figure 7 d–i. Peaks at 714.0 and 712.4 on Fe2p scan showed Fe^{III}O (ref. 26) and Fe³⁺ bound with OH (ref. 22), respectively. A peak at 726.9 showed Fe III hydroxide, peaks at 289.3 and 289.5 on C1s scan showed iron carbonate²⁴. Peaks at 285.2 and 285.1 showed the presence of carbon²⁴. O1s scan denoted the peak at 534.9 and 531.5 showed the presence of oxide of carbonate and hydroxide of iron^{25,27} respectively. XPS reveals that FeOOH present on the bare steel is changed to ferric oxides, oxides of carbonate and hydroxide due to corrosion. This study supports the observation made by FTIR and XRD.

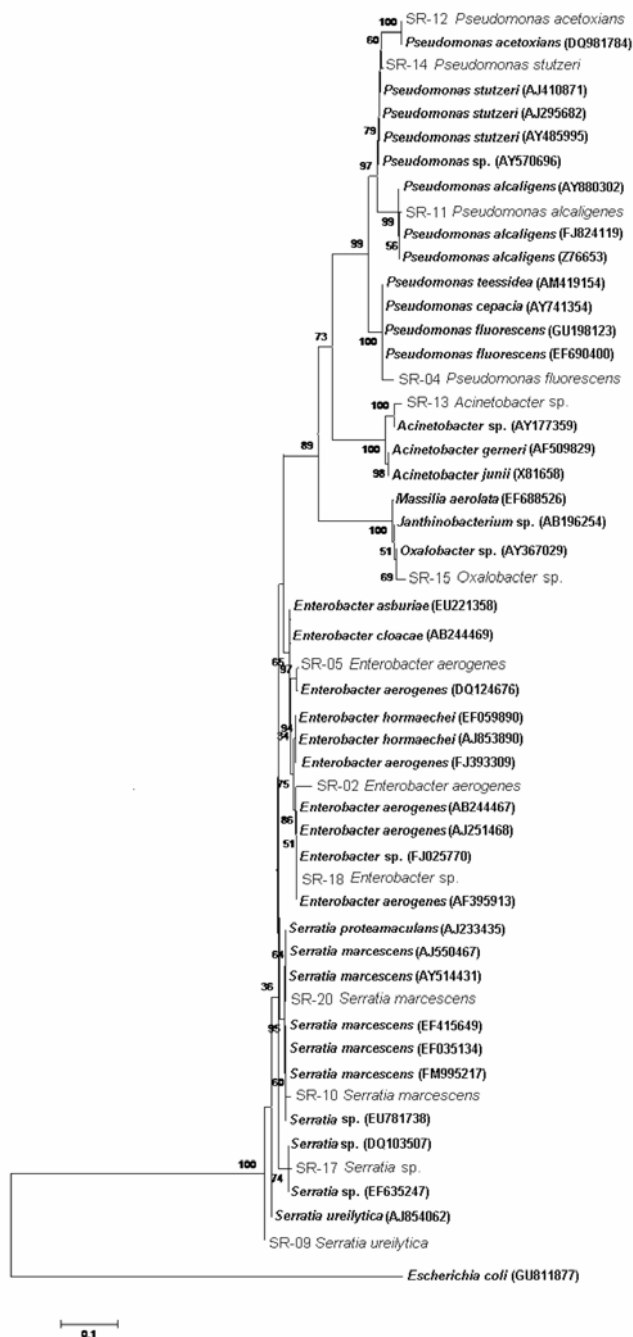


Figure 4. Neighbour-joining tree based on 16S rRNA gene sequences showing phylogenetic relationships between sequences of the phylum Proteobacteria. *E. coli* was used as the out-group sequence. Numbers at nodes indicate bootstrap values >50% from 1000 replicates. Accession numbers of the related GenBank sequences are given in parentheses. The isolate number and identified bacterial species are given in the normal face fonts. The scale bar indicates sequence divergence.

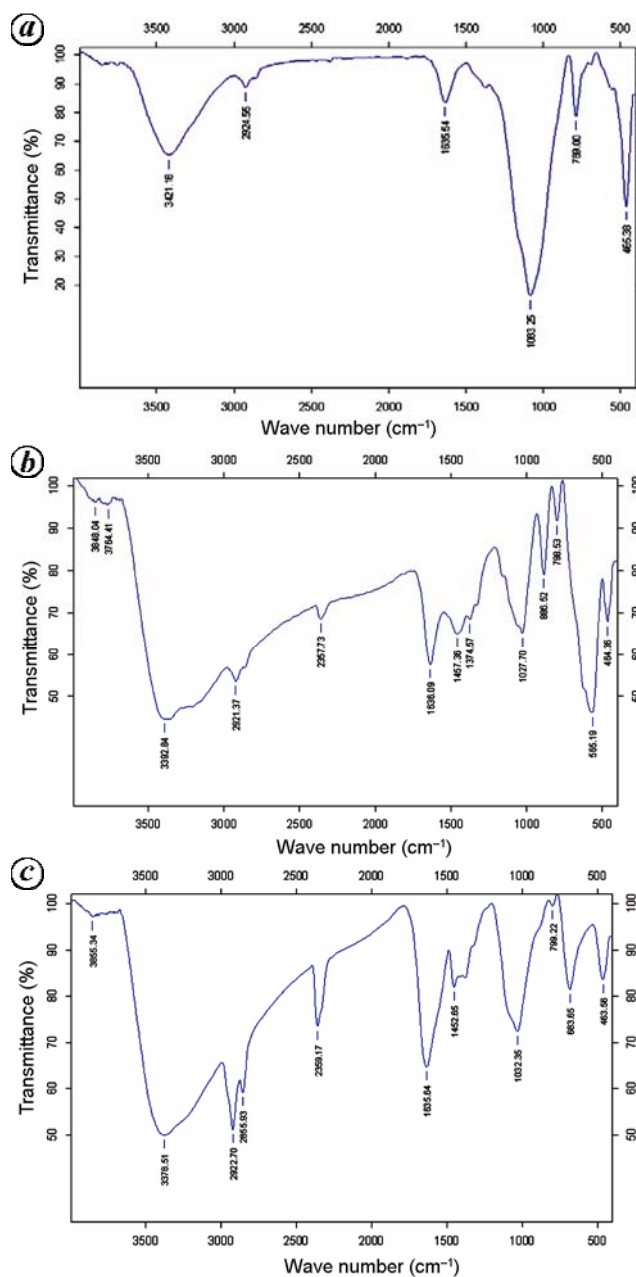


Figure 5. FTIR spectrum for a, Bare steel; b, Corrosion product collected from RIT, and c, ERC.

Electrochemical studies

Weight loss experiment: Weight loss of rail in the presence and absence of bacteria is presented in Table 4. In the control system without bacteria and urea, the weight loss was 46.5 mg and corrosion rate was 0.055 mmpy. In presence of bacteria and urea, the weight loss was 13.45 mg and corrosion rate was 0.032 mmpy. It indicates that the corrosion rate was lower in the presence of

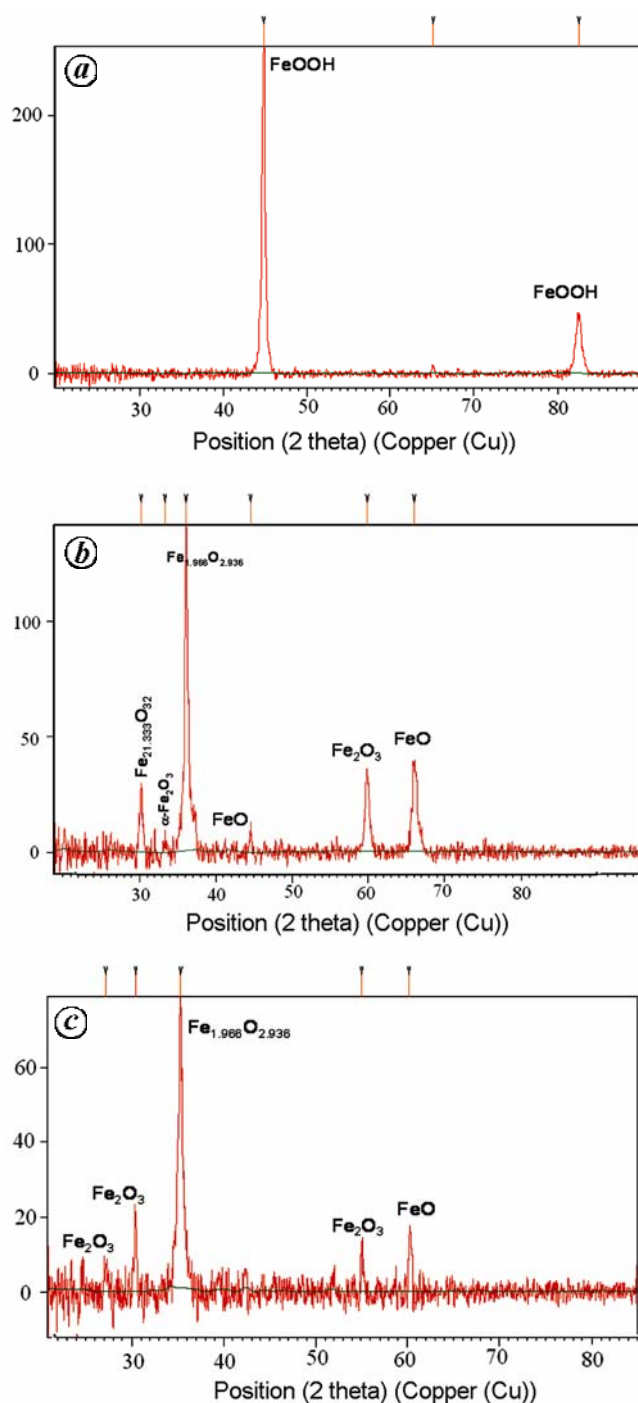


Figure 6. XRD spectrum for *a*, Bare steel; *b*, Corrosion product collected from RIT, and *c*, ERC.

urea and bacteria, when compared to control which is due to the adsorption of bacteria with the organic complex. Urea also acts as a good inhibitor. The reduction of oxygen by bacteria in the electrolyte is also one of the reasons for the low corrosion rate.

Polarization: Figure 8 shows the polarization curve for steel in presence/absence of bacteria. The corrosion current for control system was $7.96 \mu\text{A}/\text{cm}^2$ whereas in the presence of bacteria, the current was $12.47 \mu\text{A}/\text{cm}^2$ (represented in Table 5). The corrosion potential for control system was -728 mV versus SCE and in presence of bacteria the value was -789 mV versus SCE on 7th day. The anodic curve shifted to right side which indicates that the bacteria enhances anodic reactions on 7th day. The enhancement of i_{corr} is also due to the contribution of bacteria to corrosion of steel. The enhancement of anodic reaction is due to the heterogeneity of bacterial attachment on rails and metabolic activity of bacteria on rails. The polarization studies contradict the weight loss studies. The nature of film formation and oxygen consumption in the electrolyte and surface of the metal by the biofilm determine the electrochemical behaviour of rail steel. The real corrosion behaviour reflects in the weight loss while removing the corrosion product. The lower weight loss in presence of bacteria is due to oxygen consumption by bacteria in the electrolyte and formation of biofilm on the metal surface. Moreover, oxygen reduction by bacteria reflects in the cathodic reduction current. The anodic current is high in the presence of bacteria which determines the weight loss.

Impedance: The charge transfer resistance and double layer capacitance were derived from the impedance measurement and are represented in Table 5 and Figure 9. In presence of bacteria, the resistance R_{ct} value was $2.45 \text{ k ohm cm}^{-2}$, where the charge transfer resistance for the control system was $1.02 \text{ k ohm cm}^{-2}$. It reveals that the formation of a biofilm reduces corrosion by way of increasing resistance. Nyquist plot indicates the activation control reaction. When the rail sample was evaluated at low AC perturbations, the biofilm give protection to the rails. In presence of bacteria, two loops can be noticed; the first loop indicates the biofilm formation on the rails. However, at higher anodic potentials in polarization experiments, the biofilm is no longer able to protect the base material. Hence, even though the resistance is higher in presence of bacteria, the systems are controlled by anodic reactions.

Table 4. Weight loss study for rail steel

System	Weight loss (mg)	Corrosion rate (mmpy)
Control	46.5	0.055
Experiment	13.45	0.032

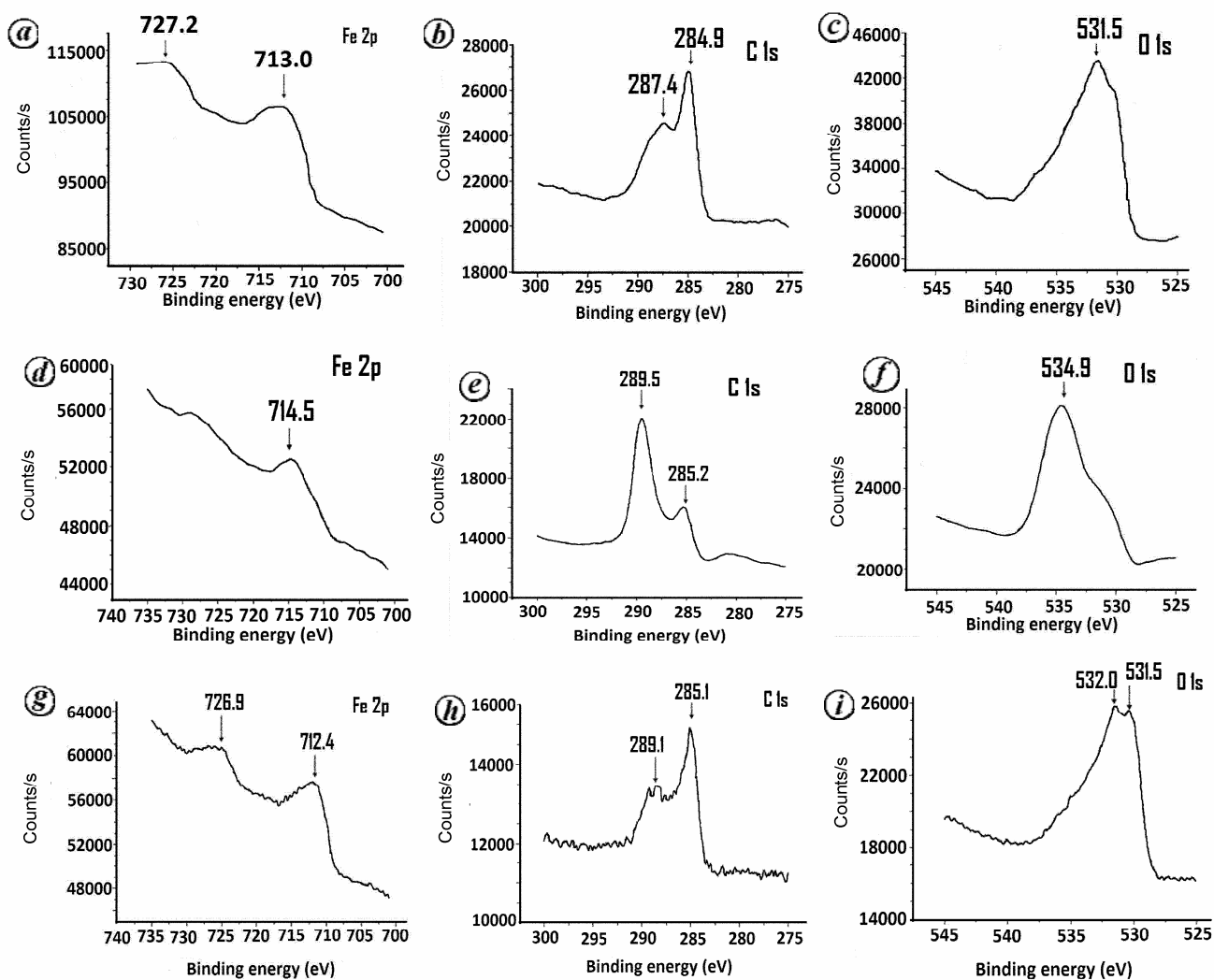


Figure 7. XPS spectrum for *a-c*, Bare rail; *d-f*, Corrosion product collected from ERC, and *g-i*, RIT.

Table 5. Polarization and impedance measurements for rail steel

Sample	E_{corr} (mV/SCE)	I_{corr} ($\mu\text{A}/\text{cm}^2$)	Corrosion rate (mmpy)	Resistance (R_{ct})
Control	-728	7.96	0.18	1.021 k ohm
Experiment	-789	12.47	0.28	2.459 k ohm

The weight loss also shows low corrosion rate in presence of bacteria. It can be assumed that urea is a good anodic inhibitor which suppresses the corrosion rate. But the heterogeneity of the biofilm in dry and wet conditions of rail surface enhances the corrosion in open atmosphere. It can be inferred that the biofilm formation in natural environment gives temporary protection, where the presence of chloride and other ions enhances the corrosion by breaking the temporary protective biofilm. In the weight loss study, the pH of the synthetic urine was 9.2 on the 7th day. Generally, ureolytic bacteria hydrolyses urea and produce carbonic acid and ammonia². At

physiological pH, the carbonic acid proton dissociates and the ammonia molecules equilibrate with water to become protonated, resulting in a net increasing pH. The first molecule of carbonic acid may encourage the growth of iron and manganese oxidizers. It is also well known that manganese and iron oxidizers prefer low pH environment. It is possible that the heterogeneity of biofilm may create differential pH environment on the metal surface and encourage the proliferation of ureolytic bacteria, iron bacteria and manganese oxidizing bacteria. The higher pH enhances calcium deposition subsequently. On the basis of these results, it can be concluded that the

evolution of higher pH (OH^- ions) encourages a thin less crystalline film on the metal surface. Further study of the salt fog experiment is under progress for proposing mechanism for bacteria on rails.

Nucleotide sequence accession numbers

The nucleotide sequences coding the gene 16S rRNA has been submitted to Genbank with the accession numbers HM475270–HM475289.

Conclusion

In this study, 20 bacterial strains of heterotrophic bacteria, manganese oxidizers, iron bacteria and ureolytic bacteria have been identified on rails by molecular technique. Since sulphate was absent on the surface, acid producers and sulphate reducers could not be noticed on the rails. The attachment of rod- and cocci-shaped bacteria on rails have been noticed. Surface analysis revealed that the FeOOH on the bare steel is changed to ferric oxides,

oxides of carbonate and hydroxide due to bacterial corrosion. The weight loss indicates that the corrosion rate was lower in presence of bacteria when compared to the control. Polarization indicates the enhancement of the anodic reaction in presence of bacteria. When the rail sample was tested at low AC perturbations, biofilm provided protection to the rails. The biofilm is no longer able to protect the bare material at higher anodic potentials. The heterogeneity of film formation and oxygen consumption in the electrolyte and surface of the metal determine the electrochemical behaviour of rail steel. The ureolytic bacteria produces carbonic acid and a second molecule of ammonia during metabolic activity which may create differential pH on the metal surface and accelerate the corrosion process. It can be concluded that the heterogeneity of the biofilm and the dry and wet conditions of the rail surface enhance the corrosion in open atmosphere.

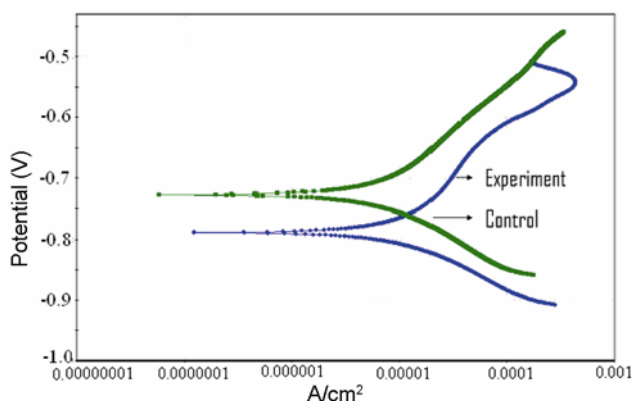


Figure 8. Polarization curve for steel in presence and absence of bacteria for seven-day exposure.

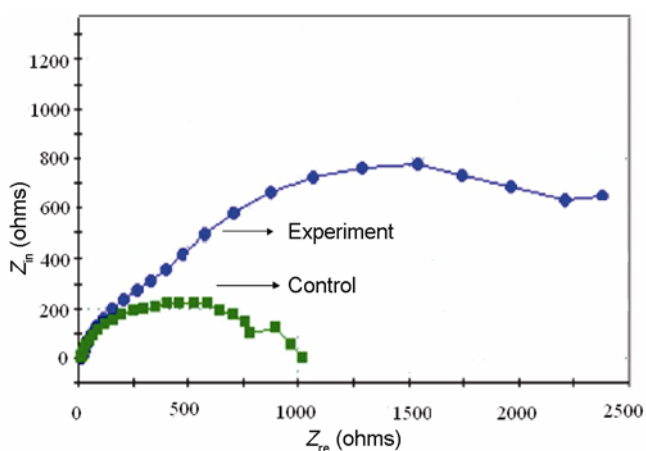


Figure 9. Impedance curve for steel in presence and absence of bacteria for seven-day exposure.

1. Robles Hernandez, F. C., Plascencia, G. and Koch, K., Rail base problem for North American transit systems. *Eng. Fail. Anal.*, 2009, **16**, 281–294.
2. Maruthamuthu, S., Muthukumar, N., Natesan and Palaniswamy, N., Role of air microbes on atmospheric corrosion. *Curr. Sci.*, 2008, **94**(3), 10.
3. Mobley, H. L. T. and Hausinger, R. P., Microbial ureases: significance, regulation, and molecular characterization. *Microbiol. Rev.*, 1989, 85–108.
4. Holt, J. G., Kreig, N. R., Sneath, P. H. A. and Stanely, J. T., In *Bergey's Manual of Determinative Bacteriology* (ed. Williams, S. T.), Williams and Wilkins, Baltimore, 1994.
5. Ausubel, F. M., Brent, R., Kingston, R. E., Moore, D. D., Seidelman, J. G. and Struhl, K. E., *Current Protocols in Molecular Biology*, Wiley, New York, 1988.
6. Weisburg, W. G., Barns, S. M., Pelletier, D. A. and Lane, D. J., 16S ribosomal DNA for phylogenetic study. *J. Bacteriol.*, 1991, **173**, 697–703.
7. Altschul, S. F., Gish, W., Miller, W., Myers, E. W. and Lipman, D. J., Basic local alignment search tool. *J. Mol. Biol.*, 1990, **215**, 403–410.
8. Larkin, M. A. *et al.*, Clustal W and Clustal X version 2.0. *Bioinformatics*, 2007, **23**, 2947–2948.
9. Kimura, M. A., Simple method for estimating evolutionary rate of base substitutions through comparative studies of nucleotide sequences. *J. Mol. Evol.*, 1980, **16**, 111–120.
10. Tamura, K., Dudley, J., Nei, M. and Kumar, S., MEGA4: Molecular Evolutionary Genetics Analysis (MEGA) software version 4.0. *Mol. Biol. Evol.*, 2007, **24**, 1596–1599.
11. Hillis, D. M. and Bull, J. J., An empirical test of bootstrapping as a method for assessing confidence in phylogenetic analysis. *Syst. Biol.*, 1993, **42**, 182–192.
12. Campanella, J. J., Bitincka, L. and Smalley, J., MatGAT: an application that generates similarity/identity matrices using protein or DNA sequences. *BMC Bioinformatics*, 2003, **4**(29), 1–4.
13. Torzewska, A., Staccek, P. and Rózalcki, A., Crystallization of urine mineral components may depend on the chemical nature of *Proteus* endotoxin polysaccharides. *J. Med. Microbiol.*, 2003, **52**, 471–477.
14. Treseder, R. S., Barboian, R. and Munger, C. G., *NACE Corrosion Engineer's Reference Book*, 1980, 2nd edn, pp. 78–79.
15. Rajasekar, A., Ganesh Babu, T., Karutha Pandian, S., Maruthamuthu, S., Palaniswamy, N. and Rajendran, A., Biodegradation and corrosion behavior of manganese oxidizer *Bacillus cereus*

RESEARCH ARTICLES

- ACE4 in diesel transporting pipeline. *Corrosion Sci.*, 2007, **49**, 2694–2710.
16. Panda, B., Balasubramaniam, R. and Dwivedi, G., On the corrosion behaviour of novel high carbon rail steels in simulated cyclic wet–dry salt fog conditions. *Corrosion Sci.*, 2008, **50**, 1684–1692.
 17. Braissant, O., Verrecchia, E. P. and Aragno, M., Is the contribution of bacteria to terrestrial carbon budget greatly underestimated? *Nat. Sci.*, 2002, **89**, 366–370.
 18. Knorre, H. and Krumbein, W., Bacterial calcification. In *Microbial Sediments* (eds Riding, R. R. and Awramik, S. M.), Springer-Verlag, Berlin, Heidelberg, 2000, pp. 25–31.
 19. Allam, I. M., Arlow, J. S. and Saricimen, H., Initial stages of atmospheric corrosion of steel in the Arabian Gulf. *Corrosion Sci.*, 1991, **32**(4), 417–432.
 20. He, Z., Honeycutt, C. W. and Griffin, T. S., Comparative Investigation of sequentially extracted phosphorus fractions in a sandy loam soil and a swine manure. *Commun. Soil Sci. Plant Anal.*, 2003, **34**(11), 1729–1742.
 21. Robert, M. S., Francis, X. W. and David, J. K., *Spectrometric Identification of Organic Compounds*, John Wiley, 2005, 7th edn, pp. 73–108.
 22. Muthukumar, N., Mohanan, S., Maruthamuthu, S., Subramanian, P., Palaniswamy, N. and Raghavan, N., Role of *Brucella* sp. and *Gallionella* sp. in oil degradation and corrosion. *Electrochem. Commun.*, 2003, **5**, 421–425.
 23. Gusmano, G., Montanari, R., Kaciulis, S., Mezzi, A., Montesperelli, G. and Rupprecht, L., Surface defects on collection coins of precious metals. *Surf. Interface Anal.*, 2004, **36**, 921–924.
 24. Deodshmukh, V. *et al.*, X-ray photoelectron spectroscopic analyses of corrosion products formed on rock bolt carbon steel in chloride media with bicarbonate and silicate ions. *Corrosion Sci.*, 2004, **46**, 2629–2649.
 25. Heuer, J. K. and Stubbins, J. F., An XPS characterization of FeCO₃ films from CO₂ corrosion. *Corrosion Sci.*, 1999, **41**, 1231–1243.
 26. Albert, O., Janos, K. and Imre, K., XPS investigations on the feasibility of isomorphous substitution of octahedral Al³⁺ for Fe³⁺ in Keggin ion salts. *Phys. Chem. Chem. Phys.*, 1999, **1**, 2565–2568.
 27. Enikeev, E. Kh., Feoktistov, A. K., Panov, M. K. and Krasheninnikova, I. M., Chemical composition and structure of the surface layers-products of interaction between steel 3 and hostile aqueous environment: the effect of the environment. *Russian J. Electrochem.*, 2000, **36**(4), 378–386.

ACKNOWLEDGEMENTS. We thank Mr R. Ravishanker, Mrs T. Nalini, Miss G. V. M. Krithika and Miss S. Krithika for their assistance in the utilization of the facilities SEM, FTIR, XPS and XRD in the Instrumentation Division, CSIR-CECRI, India respectively. We also thank the Southern Railways for entrusting study to CSIR-CECRI, Karaikudi and associated assistance.

Received 2 July 2010; revised accepted 9 December 2010

CURRENT SCIENCE Display Advertisement Rates

India

No. of insertions	Size	Tariff (Rupees)					
		Inside pages		Inside cover pages		Back cover page	
		B&W	Colour	B&W	Colour	B&W	Colour
1	Full page	10,000	20,000	15,000	25,000	20,000	30,000
	Half page	6,000	12,000	–	–	–	–
6	Full page	50,000	1,00,000	75,000	1,25,000	1,00,000	1,50,000
	Half page	30,000	60,000	–	–	–	–
12	Full page	1,00,000	2,00,000	1,50,000	2,50,000	2,00,000	3,00,000
	Half page	60,000	1,20,000	–	–	–	–

Other countries

No. of insertions	Size	Tariff (US\$)					
		Inside pages		Inside cover pages		Back cover page	
		B&W	Colour	B&W	Colour	B&W	Colour
1	Full page	300	650	450	750	600	1000
	Half page	200	325	–	–	–	–
6	Full page	1500	3000	2250	3500	3000	5000
	Half page	1000	2000	–	–	–	–

Note: For payments towards the advertisement charges, Cheques (local) or Demand Drafts may be drawn in favour of 'Current Science Association, Bangalore'.